Hindawi
Cellular Microbiology
Volume 2022, Article ID 8738290, 9 pages
https://doi.org/10.1155/2022/8738290

Research Article

Deletion of a Putative GPI-Anchored Protein-Encoding Gene Ao*g185* Impedes the Growth and Nematode-Trapping Efficiency of *Arthrobotrys oligospora* by Disrupting Transmembrane Transport Homeostasis

Hui Peng,[1,2,3] Hengqian Lu,[1,2,3] Xinyuan Dong,[1,2,3] Xiao Liang,[1,2,3] Kangliang Sheng,[1,2,3] Jingmin Wang,[1,2,3] Xiaowei Kong,[1,2,3] Xiangdong Zha,[1,2] and Yongzhong Wang[1,2,3,4]

[1]*School of Life Sciences, Anhui University, Hefei 230601, China*
[2]*Key Laboratory of Human Microenvironment and Precision Medicine of Anhui Higher Education Institutes, Anhui University, Hefei 230601, China*
[3]*Anhui Key Laboratory of Modern Biomanufacturing, Hefei 230601, China*
[4]*Institute of Physical Science and Information Technology, Anhui University, Hefei 230601, China*

Correspondence should be addressed to Yongzhong Wang; yzwang@ahu.edu.cn

Received 5 August 2022; Revised 28 October 2022; Accepted 29 October 2022; Published 14 November 2022

Academic Editor: Sivasankar Palaniappan

Nematode-trapping fungus (NTF) is a crucial predator of nematodes, which can capture nematodes by developing specific trapping devices. However, there is limited understanding of the role and mechanism of cell surface proteins attached to the surface of mycelia or trapping cells. Here, the effects of a putative GPI-anchored protein-encoding gene Ao*g185* on the growth and nematode-trapping efficiency of *A. oligospora* were investigated. Compared to the wild-type (WT) strain, the *Δ*Ao*g185* mutant grew more slowly, exhibited a 20% decrease in conidiation, delayed conidial germination, generated fewer traps, attenuated nematode trapping efficiency, and was more sensitive to chemical stressors. Transcriptomic analysis indicated that a large number of transmembrane transport-related genes were differentially expressed between the WT and *Δ*Ao*g185* mutant strains. Ao*g185* deletion could damage the intrinsic components of the membrane and cytoskeleton. Specifically, knockout of Ao*g185* disrupted transmembrane transport homeostasis during the phagocytosis, cell autophagy, and oxidative phosphorylation processes, which were associated with the fusion of cells and organelle membranes, transport of ions and substrates, and energy metabolism. Hence, the putative GPI-anchored protein-encoding gene Ao*g185* may contribute to the lifestyle switch of NTF and nematode capture, and the effect of Ao*g185* gene on cell transmembrane transport is considered key to this process. Our findings provide new insights into the mechanism of Ao*g185* gene during the process of nematode trapping by NTF.

1. Introduction

Plant-parasitic nematodes cause approximately >$150 billion worth of damage to agriculture each year worldwide [1]. The nematode-trapping fungus (NTF) is a natural predator of nematodes that forms specific mycelial structures called trapping devices to prey and digest nematodes [2]. The trap also belongs to a mechanism of fungus, allowing it to switch from saprophytic to predacious lifestyles [3]. Over the last 30 years, our understanding of the mechanisms of trapping and killing nematodes by NTF has improved tremendously, and the switch of strains from saprophytic to parasitic lifestyles has proven to be a key for trapping and killing nematodes [4]. In recent years, the identification of critical genes, proteins, metabolic pathways, and biological processes involved in the switch of the NTF lifestyle has become a popular research topic [5]. Compelling evidence suggests that multiple signaling pathways are activated in fungi by its nematode prey to further modulate downstream genes involved in distinct cellular processes, including catabolism, energy metabolism, transmembrane transport, biosynthesis of the cell wall and adhesive proteins, peroxisome biogenesis, stress responses, and cell division [6]. Therefore, the switch of strains from saprophytic to parasitic lifestyles is a global metabolic reprogramming. However, the critical factors affecting this reprogramming remains unknown.

Previous multiomics analyses revealed that many adhesion-associated protein-encoding genes were detected in the NTF genome, most of which were upregulated during the formation of traps [4, 7]. Liang et al. proved the important role of cell surface adhesins in the formation of traps and the lifestyle switching in NTF at the molecular level through the knockout of the adhesion-associated protein-encoding gene *Mad1* in *Arthrobotrys oligospora* [8]. These studies indicate that the functional cell surface proteins are important for trapping nematodes. Glycosylated phosphatidylinositol-anchored proteins (GPI-APs) are a class of proteins that can be anchored to the eukaryotic cell membrane surface through the GPI structure at the carboxyl end [9–12]. Previous research has suggested that GPI-APs have important impacts on fungal adhesion, morphological transformation, and cell wall synthesis and play a vital role in mediating the adhesion process between fungi and host cells [13].

A. oligospora is a well-characterized NTF that captures nematodes with specialized traps. In this study, a putative GPI-AP gene Ao*g185* was identified in *A. oligospora*, and the effects of Ao*g185* on the lifestyle switch were assessed through gene knockout experiments. The potential mechanisms by which Ao*g185* affects cell growth and trapping efficiency were then revealed using comparative transcriptomics analysis.

2. Materials and Methods

2.1. Strains, Plasmids, and Culture Conditions. A. oligospora was supplied by American Type Culture Collection (ATCC 24927; VA, USA), and its fungal mutant strains were cultured on potato dextrose agar (PDA) medium in an incubator at 28°C. Plasmid pUC19 (TaKaRa Bio, Shiga, Japan) was maintained in *E. coli* strain DH5*α*. Plasmid pUC57-HygB was synthesized by General Biosystems (Anhui, China) for recombinant plasmid construction. Fungal mycelia were harvested into liquid TG (1% tryptone and 1% glucose) medium. The 0.75% agar TB3 (200 g sucrose, 3 g tryptone, and 3 g yeast extract diluted to 1 L) medium was utilized for protoplast regeneration. TYGA (1% tryptone, 1% glucose, 0.5% yeast extract, and 0.5% molasses) and CMA (17 g/L corn meal agar) were employed to determine the phenotypic traits of *A. oligospora* and mutant strains. *Caenorhabditis elegans* was maintained on NGM (NaCl, 0.3 g; peptone, 0.25 g; agar powder, 1.7 g; 1 mol/L $MgSO_4$, 0.1 mL; 1 mol/L $CaCl_2$, 0.1 mL; 5 mg/mL cholesterol ethanol solution, 0.1 mL; 1 mol/L KH_2PO_4-K_2HPO_4 buffer (pH 6.0), 2.5 mL per 100 mL) medium at 20°C.

2.2. Sequences and Phylogenetic Analysis of Aog185. The amino acid sequence of Ao*g185* was downloaded from GenBank (https://www.ncbi.nlm.nih.gov/). Conserved functional domains and partial biochemical properties were analyzed using the InterPro (http://www.ebi.ac.uk/interpro/) and pI/Mw tool (http://www.expasy.ch/tools/pi-tool.html), respectively. The orthologous proteins of GPI-anchored cell surface containing the actin-depolymerizing factor (ADF)/cofilin domain from different fungi were retrieved from GenBank, and a neighbor-joining tree for ADF/cofilin was established with Mega 7.0 software [14].

2.3. Deletion of Aog185 Gene. Ao*g185* gene was knocked out by homologous recombination as previously described [15]. PCR amplification was performed on 2 flanking fragments (a 2000-bp downstream and 2000-bp upstream) using the paired primers (Supplementary Table S1). The hygromycin B (HygB) resistance gene cassette in the PUC57-HygB plasmid was also amplified. The two homologous fragments, HygB cassette and linearized pUC19 vector were inserted into *E. coli* DH5*α*.

The combined plasmid pUC19-Ao*g185*-HygB was then transformed into *A. oligospora* protoplast as previously described [16, 17]. The presence of HygB resistance gene in the transformants was detected using the agar containing hygromycin B (150 μg/mL). The putative transformants were verified by PCR assays using the specific primer pairs (Supplementary Table S1) and then sequenced.

2.4. Mycelial Growth, Conidiation, and Germination. Wild-type (WT) and mutant strains were maintained on CMA plates at 28°C for 6 days, and a 0.8 cm diameter hyphal disk was then cultured on PDA, TYGA, and CMA plates at 28°C for 6 days to assess the diameter of fungal growth every day at a fixed time point. The number of conidia (sterile water-rinsed, collected conidia of the previous CMA plates) and their conidial germination rates were determined and observed on water agar plates. All experiments were carried out in triplicate.

2.5. Stress-Tolerance Analysis. To determine the effects of both WT and mutants on the resistance of *A. oligospora* to chemical stressors, the colonies initiated with hyphal-mass disks (0.8 cm in diameter) were incubated for 6 days at 28°C on TG medium alone (control) or supplemented with chemical stressors as follows: (1) 0.1, 0.2, and 0.3 M NaCl for osmotic stress; (2) 0.01%, 0.02%, and 0.03% SDS for cell wall perturbation; (3) 5, 10, and 15 mM H_2O_2 for oxidative stress [16, 18]. The diameter and hyphal morphologies of each colony were examined, and the suppression ratio was calculated according to the

$$\text{Suppression ratio}(\%) = \frac{(R_0 - R_{cs})}{R_0} \times 100\%, \tag{1}$$

where R_0 is the diameter of each colony grown for six days in the native TG plates supplemented without any chemical stressors, and R_{cs} is the diameter of each colony grown for six days in the TG plates supplemented with chemical stressors at different concentrations. All experiments were conducted in triplicate.

2.6. Trap Formation and Bioassays. To evaluate whether A*og185* can regulate trap formation in *A. oligospora*, both WT and mutant strains were cultured on water agar (WA, 15%) medium for 3 days at 28°C. Approximately 500 nematodes were then introduced into the cultures. After 8 h of incubation, the traps and captured nematodes in each plate were determined using an inverted fluorescence microscope and counted at specific time points [4].

2.7. Transcriptomic Analysis. The LNAAM was used as the culture medium for the shake-flask cultivation of *A. oligospora* prior to transcriptomic analysis. The hyphae of WT and A*og185* knockout strains were harvested at 0, 18, and 36 h after adding the nematode extract (NE) liquid. The collected hyphae were immediately frozen using liquid nitrogen and kept in a -80°C refrigerator. Three biological repeats were performed at each time point. The samples were transferred to the Shanghai Majorbio for transcriptome sequencing using an Illumina Novaseq 6000 sequencer. Statistical methods, such as fastx_toolkit, Sickle, SeqPrep, and fastp, were used to perform statistics and quality control of the tested sequences.

The clean reads were mapped by the complete reference using Bowtie2 v2.4.1 (http://bowtie-bio.sourceforge.net/index.shtml) [19]. RSEM v1.3.3 (https://www.biostat.wisc.edu/~cdewey/), kallisto v0.46.2, and Salmon v1.3.0 were used to measure the expression level of each gene [20]. Using the gene expression level of WT strain as a control, differentially expressed genes (DEGs) were detected in A*og185* mutant strain using the DESeq2 tool v1.24.0, $\log2\,FC \geq 1$ and $p\,\text{adjust} < 0.05$ were considered DEGs. GO annotation of genes was performed using the eggNOG database (version 5.0). Phyper (a function of the R program) and Goatools were used for the GO enrichment analyses.

2.8. Statistical Analysis. The values are presented as mean ± standard deviation. SPSS software v23.0 (SPSS Inc., IL, USA) was employed to process the data in this study, and the *T* test was used to analyze and compare the differences between the groups. Levels of statistical significance were set at $^{*}p < 0.05$ and $^{**}p < 0.01$. Prism 8.0 (GraphPad, CA, USA) was employed for image construction.

3. Results

3.1. Sequences and Phylogenetic Analysis of Aog185 in A. oligospora. Aog185 protein containing 1102 amino acids (molecular mass = 117.6 kDa) was identified in *A. oligospora* as an ortholog of GPI-anchored cell surface protein at the ADF/cofilin domain of *Glarea lozoyensis* and *Pyronema omphalodes*. Two conserved domains, ADF-H (IPR002108) and cofilin_ADF (PF00241), belonging to the ADF-H/gelsolin-like domain superfamily (IPR029006), were predicted in Aog185 protein through InterProScan. The A*og185* sequences were found to be more identical (68–78.9%) to those of NTF orthologs such as *Drechslerella stenobrocha* (78.9%), *Drechslerella brochopaga* (76.7%), and *Dactylellina cionopaga* (68%) than those of other filamentous fungi such as *Aspergillus aculeatinus* (37.9%) and *Glarea lozoyensis* (40.6%). A phylogenetic tree was constructed based on the homologous Aog185 protein of different fungi. The results showed that Aog185 proteins from these fungi could be clustered into two clades (A-*I* and A-II). The orthologous Aog185 sequences from three NTF species were grouped as A-II, while other fungi belonged to A-*I* (Figure 1).

3.2. Construction of Knockout Plasmids and Verification of ΔAog185 Mutant. To ligate the downstream and upstream homology arms of A*og185* (2000 bp each) and HygB resistance cassette (2121 bp), the seamless ligation primers were designed using the SnapGene software (Table S1). Figure S1 displays the principle of A*og185* gene knockout via homologous recombination. The linearized pUC19 cut by *Nde*I and *Pci*I was first verified as the backbone vector for infusion cloning, and then transformed into *E. coli*. Seven clones were randomly chosen for PCR amplification using the corresponding primers (A*og185*-1F/1R, A*og185*-3F/3R, or HygB-2F/2R), and PCR data revealed that all 3 fragments were successfully ligated into the linearized pUC19. Five clones were simultaneously chosen for PCR verification using the respective primer A*og185*-1F/3R, resulting in a 6121-bp amplicon, followed by DNA sequencing. The results confirmed that the knockout plasmid pUC19-A*og185*-HygB was successfully constructed.

After transforming pUC19-A*og185*-HygB into the protoplasts of *A. oligospora*, the transformants were chosen on TYGA plates containing 150 μg/mL HygB. Mycelial PCR indicated that an amplicon of 3114 bp was amplified from the *Δ*A*og185* mutant, whereas a 4952-bp amplicon was generated from the WT strain (Figure S2A). For comparison, both 3114-bp and 4952-bp amplicons were produced for false-positive transformants, where A*og185* had been knocked out partially. As displayed in Figure S2A, only seven completely positive *Δ*A*og185* mutants (No. 2, 3, 5, 11, 14, 16, and 26) were obtained. These *Δ*A*og185* mutants were subsequently cultured on nonantibiotic TYGA medium for three generations. Mycelial PCR amplification and sequencing of PCR product were also carried out to confirm the correct transformants. As shown in Figure S2B, A*og185* gene in all these seven transformants was knocked out.

3.3. Effect of Aog185 on Conidiation and Growth. Compared to the WT strain, the growth of mutant strain was significantly lower on the CMA, TYGA, and PDA plates (Figure 2). In addition, the disruption of A*og185* gene could reduce conidiation. Conidial production in the *Δ*A*og185* mutant (1.73×10^5 conidia per plate) significantly reduced compared to that in the WT strain (4.80×10^5 conidia per plate) (Figure S3A). After incubation on WA plates, the conidial germination rates of WT were remarkably increased compared to *Δ*A*og185* mutant both at 2 h (61.45% and 55.64% for WT and *Δ*A*og185* mutant, respectively) and 4 h (84.35% and 75.33% for WT and *Δ*A*og185* mutant, respectively). Both WT and mutant strains showed 100% conidial germination rate after

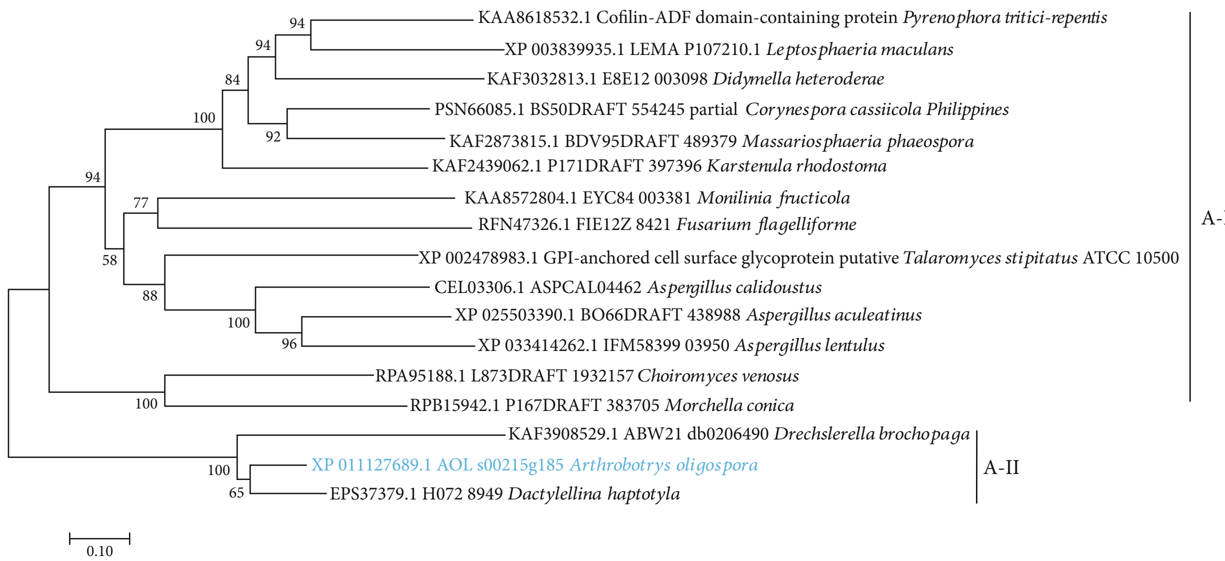

Figure 1: Phylogenetic analysis of homologous Aog185 protein from different fungi based on their deduced amino acid sequences. GenBank accession number is given. These proteins were clustered into 2 groups (A-I and A-II).

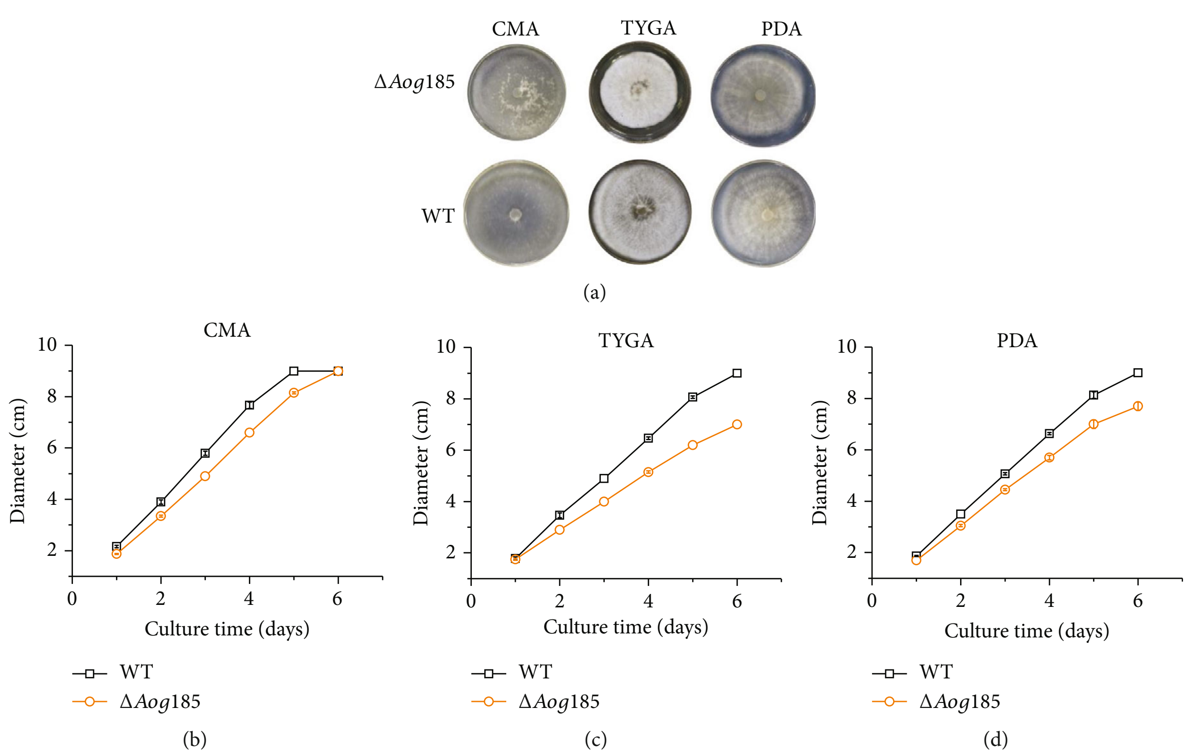

Figure 2: Comparison of mycelial growth between the WT and *ΔAog185* mutant strains. Colonies from the WT and *ΔAog185* mutant strains were grown on PDA, TYGA, and CMA media for 6 days at 28°C (a). Mycelial growth rates of the WT and *ΔAog185* mutant strains on CMA (b), TYGA (c), and (d) PDA plates. $^{*}p < 0.05$ and $^{**}p < 0.01$.

incubation for 12 h (Figure S3B). Thus, *Aog185* gene plays crucial roles in enhancing conidiation, conidial germination, and growth of *A. oligospora*.

3.4. Vital Role of Aog185 in Stress Responses. The responses of WT and *ΔAog185* mutant strains to three types of chemical stressors, such as an osmotic agent (NaCl), a cell wall-perturbing agent (SDS), and an oxidant (H_2O_2), were also studied. As compared to the native TG media without supplement of any chemical stressors, the suppression ratio of *ΔAog185* mutant was significantly higher than the WT strain in TG media supplemented with NaCl at low concentrations ranging from 0.1 M to 0.2 M, whereas the suppression ratios for both the strains at high NaCl concentration

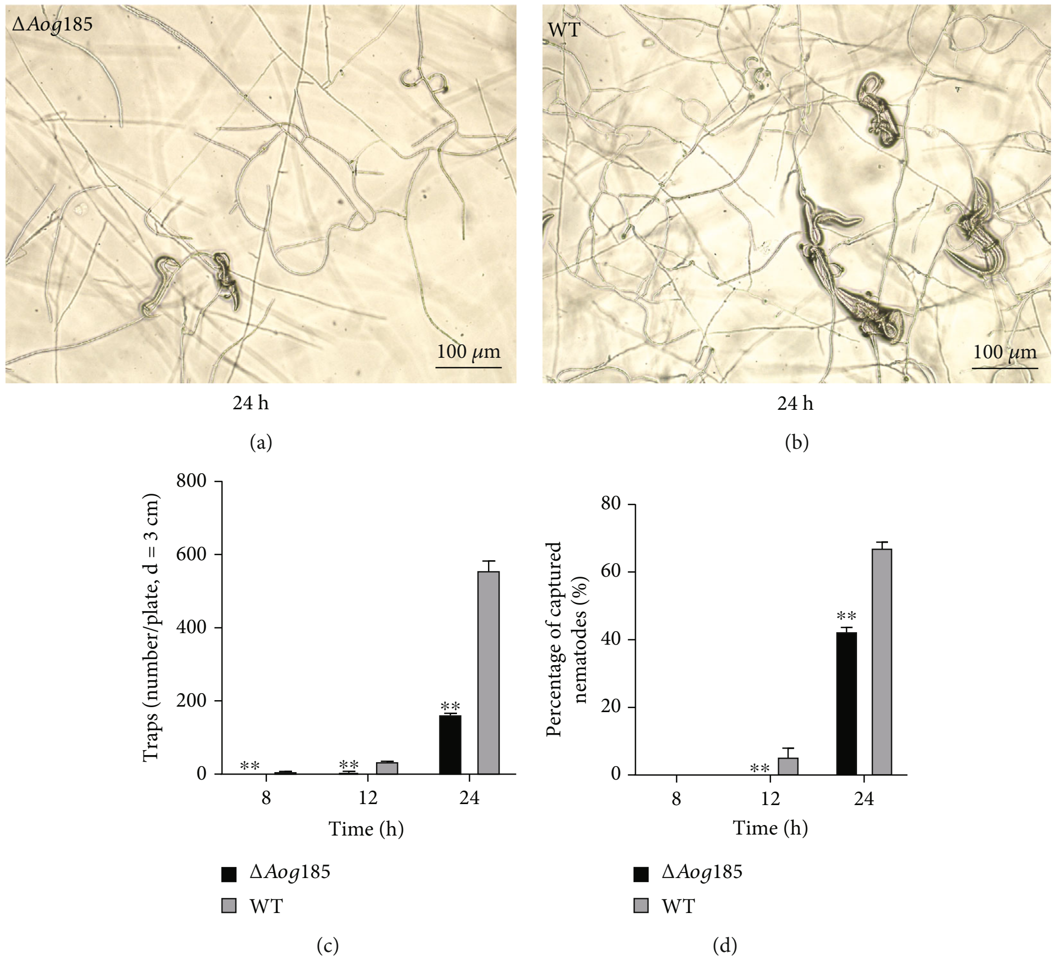

Figure 3: Comparisons of trap formation and nematicidal activities between the WT and *ΔAog185* mutant strains. (a, b) Representative images of the trap formation and nematode trapping of the WT and *ΔAog185* mutant strains after addition of nematodes for 24 h. (b) The numbers of nematode-induced traps generated by the WT and *ΔAog185* mutant strains after addition of nematodes for 8, 12, and 24 h. (c) The percentages of nematodes captured by the WT and *ΔAog185* mutant strains after addition of nematodes for 8, 12, and 24 h. $^{*}p < 0.05$ and $^{**}p < 0.01$.

of 0.3 M were not significantly different (Figure S4A and B). Similarly, compared to the native TG media, the suppression ratio of *ΔAog185* mutant was significantly higher than the WT strain in TG plates containing >0.02% SDS, whereas both the strains showed similar suppression ratios at 0.03% SDS concentration (Figure S4C and D). As for chemical stressor H_2O_2, the WT strain and *ΔAog185* mutant had similar suppression ratios at TG plates supplemented H_2O_2 at concentrations ranging from 5 mM to 15 mM (Figure S4E and F).

3.5. Aog185 Is Responsible for Trap Formation and Host Infection. Trap formation was induced by the addition of nematodes to WA plates. After 8, 12, and 24 h of incubation, traps were observed on the WT strain- and *ΔAog185* mutant-WA plates (Figures 3(a) and 4(b)). After incubation for 8 h, the WT strain began to form immature traps containing a single ring, while no trap was found on the WA plate cultured with *ΔAog185* mutant. Mature traps and 3D nets were formed after incubation for 12 and 24 h. In the plate incubation of the WT strain, approximately 11.7, 36.1, and 557.67 traps were observed after incubation for 8, 12, and 24 h, respectively. Meanwhile, only 0, 8.33, and 164.67 traps were observed in the plate where the *ΔAog185* mutant was incubated (Figure 3(c)). Moreover, the nematicidal activities of WT and *ΔAog185* mutant strains were also counted and measured at varying time points. There was no predation at 8 h after nematode addition in either strain. The WT strain captured 5.61% and 66.58% of nematodes after incubation for 12 and 24 h, respectively, whereas the *ΔAog185* mutant captured 0 and 42.33% of the nematodes at the same time points, respectively (Figure 3(d)).

3.6. Effects of Aog185 on the Transcriptomics Landscape of A. oligospora. To explore the underlying mechanisms of *Aog185*, the transcriptomic data were compared between WT and *Aog185* knockout strains at 0, 18, and 36 h after NE stimulation. The results of transcriptomic analysis showed that 26, 376, and 122 DEGs were identified at 0, 18, and 36 h, respectively. Venn analysis displayed the number of DEGs in each gene set and the overlapping relationship of genes between gene sets and identified common

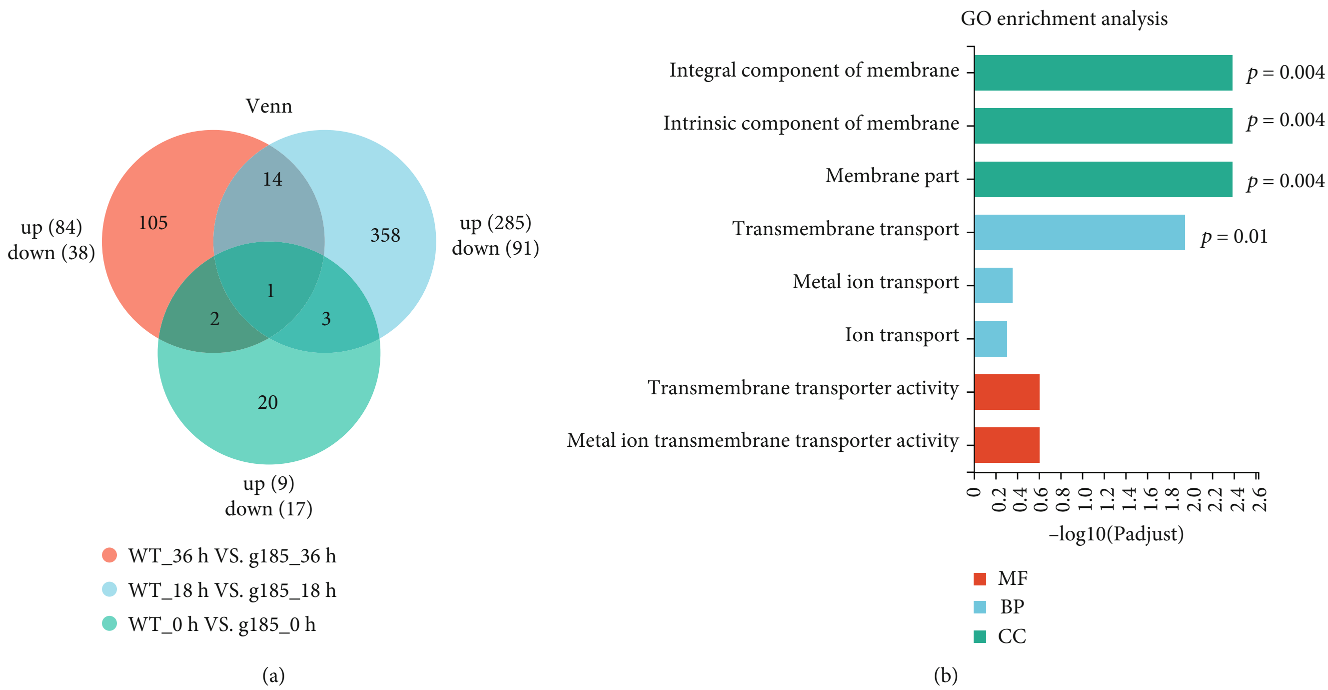

Figure 4: Transcriptome analysis reveals the role of Ao*g185* in the regulation of cell transmembrane transport. (a) Venn diagram. (b) GO enrichment analysis. The GO enrichment analyses were conducted based on the DEGs identified at 18 h. MF: molecular function; BP: biological process; CC: cellular component.

and unique genes between gene sets (Figure 4(a)). Compared with WT strains, 9, 285, and 84 genes were upregulated in Ao*g185* knockout strains at 0, 18, and 36 h, respectively, while 17, 91, and 38 genes were downregulated at the same time points, respectively ($p \leq 0.05$ and $|\log 2FC| \geq 1$). Data of these DEGs are presented in Table S6.

Based on the differential expression analysis, it was clearly observed that the effect of Ao*g185* on *A. oligospora* appeared at 18 h after NE stimulation. GO enrichment analyses were performed based on the DEGs identified at 18 h, and the data are presented in Figure 4(b). As shown in Figure 4(b), the DEGs at 18 h were mainly the integral component of membrane (p adjust < 0.05), intrinsic component of membrane (p adjust < 0.05), and membrane part (p adjust < 0.05) and involved in the biological process of transmembrane transport (p adjust < 0.05). Ao*g185* gene knockout had a significant impact on the cell transmembrane transport system, thereby regulating biological processes and pathways such as cellular oxidative phosphorylation, phagosomes, and autophagy, which are highly associated with transmembrane transport.

4. Discussion and Conclusions

In the present study, a putative GPI-anchored protein-encoding gene Ao*g185* was shown to contribute to mycelial development, hyphal growth, conidiation, 3D trap formation, pathogenicity, and stress responses. These results are consistent with the multiomics analysis results reported previously [4, 7]. However, Liang et al. pointed out that knockout of the cell surface adhesin-coding gene *AoMad1* in *A. oligopora* could promote the formation of adhesive networks [8], which are inconsistent with the results of this study. Therefore, the effects of potential cell surface proteins on NTF growth and trapping were different. The main reasons may be related to the intrinsic mechanisms of regulating cell global metabolism. Liang et al. demonstrated that the cell surface adhesin-coding gene *AoMad1* could influence NTF growth and trapping mainly through the regulation of nitrogen metabolism-related gene expression [8]. Our transcriptomics analysis indicated that the DEGs in the Ao*g185* mutant were mainly involved in transmembrane transport-related metabolic pathways and biological processes, particularly affecting cell membrane components, ion transmembrane transport-related oxidative phosphorylation, and cell reorganization-related cell autophagy and endocytosis.

In this study, Ao*g185* was identified as a GPI-AP gene, which has been shown to be involved in membrane protein transport, cell adhesion, cell wall formation, and cell surface protection [21, 22] and plays a key role in cell invasion [23]. This explains why knockout of *Aog185* inhibited the growth, development, and pathogenicity of *A. oligospora*. In addition, Aog185 protein contains the actin-depolymerizing factor (ADF)/cofilin domain, and ADF/cofilin is able to promote actin disassembly [24] and remodeling of the actin cytoskeleton [25–27]. Deletion of Ao*g185* may influence the reorganization of actin cytoskeleton, which further results in growth retardation and sporulation capacity reduction, and eventually causes cells to be more sensitive to chemical stressors. In addition, it has been reported that the actin cytoskeleton and actin-associated protein Crn1p are involved in the trap formation of *A. oligospora* [28]. ADF/cofilin proteins play important roles in controlling the temporal and spatial extent of actin dynamics, which play key roles in mediating host-pathogen interactions [29]. Ao*g185* has been proposed to be involved in the depolymerization of actin. Deletion of Ao*g185* may indirectly impede the depolymerization and remodeling of actin and ultimately decrease trap formation and nematicidal activity. Overall, the Ao*g185* mutation changes the intrinsic components of the membrane and cytoskeleton and further disrupts the homeostasis of intrinsic transmembrane transport.

Phagocytosis is a specialized process by which cells internalize large particles or a target organism. During phagocytosis, the membrane expands by cytoskeletal rearrangement to recognize foreign particles and ultimately forms a membrane-bound vacuole known as the phagosome [30]. Autophagy is an evolutionarily conserved catabolic pathway that employs lysosomes/vacuoles to degrade and recycle aging organelles and proteins in both yeast and mammalian cells. Autophagy is necessary for trap formation in *A. oligospora* [31, 32]. Both phagocytosis and cell autophagy depend on cell membrane fusion and transmembrane transport, while phagocytosis and autophagy are two important processes for microbial invasion. Chen et al. suggested that autophagy is initiated in *A. oligospora* during trap formation [33]. The effects of *Aog185* knockdown on transmembrane transport homeostasis further disturbed cell phagocytosis and autophagy, resulting in different growth and trapping rates between the Ao*g185* mutant and WT strains.

The vacuolar H^+-ATPase (vATPase) is a multisubunit enzyme that plays key roles in regulating both cell phagocytosis and autophagy processes. In the fusion of phagosome with endosomes or autophagosome with vacuolar, vATPase is the critical rate-limiting enzyme [33, 34]. The enzyme vATPase transports protons across biological membranes by utilizing the energy from ATP hydrolysis [35–37]. In addition, ATPase is a critical enzyme involved in the oxidative phosphorylation system and plays a vital role in regulating proton transmembrane transport [38]. In this study, ATPase was significantly upregulated in the Ao*g185* knockout strain, indicating that Ao*g185* affects the phagosome/autophagy pathway and ATPase mediates oxidative phosphorylation. The effect of Ao*g185* on proton transmembrane transport can further dispute cell self-cleaning and energy metabolic homeostasis and regulation of cell growth, trapping, and stress responses.

Our transcriptomics analysis also found that some genes were associated with the mitogen-activated protein kinase (MAPK) pathway [39–41] and mitophagy [42, 43], thereby regulating the adaptation of cells to environmental stress and development of morphology [44]. The DEGs also significantly changed in the *Aog185* knockout strain, including PBS2 and myotubularin-related phosphatase (MTMR) 6_7_8. PBS2 has been identified earlier in genetic screening for polymyxin B resistance genes, which integrates with MAPK pathways and is involved in stress signal transmission [45]. MTMR is associated with autophagosome formation, and knockdown of MTMR3 increases autophagosome formation [46]. MTM1, MTMR1-4, MTMR6-8, and MTMR14 are phosphatidylinositol 3-phosphatases that dephosphorylate the D-3 positions of PI(3)P and PI(3,5)P_2 in vitro [47, 48]. MTMR6_7_8 (Ymr1p) is a yeast myotubularin-related PI(3)P phosphatase that plays an essential role in regulating phosphatidylinositol 3-phosphate [49]. Our study showed that MTMR6_7_8 was significantly downregulated after Ao*g185* knockout, indicating that Ao*g185* is involved in the autophagy pathway, phosphatidylinositol signaling system, and inositol phosphate metabolism in *A. oligospora*.

Data Availability

The data used to support the findings of this study are included within the supplementary information file.

Conflicts of Interest

The authors declare that there is no conflict of interest regarding the publication of this paper.

Acknowledgments

This research was funded by the Outstanding Talents Program of Anhui University, China (Y.W.), Open Fund for Discipline Construction, Institute of Physical Science and Information Technology, Anhui University (Y.W.), and Natural Science Foundation of China (Y.W., grant numbers: 31470218 and 31770066).

Supplementary Materials

Figure S1: the principle of construction of gene knockout plasmid of Ao*g185*. Figure S2: screening and verification of *Δ*Ao*g185* transformants. Figure S3: comparison of conidiation and conidial germination rates between the WT strain and the *Δ*Ao*g185* mutant. Figure S4: comparison of stress tolerance of *A. oligospora* to osmotic agents, cell wall-perturbing agents, and oxidative agents. Table S1: list of primers used in this study. Table S2: quality check of total RNA. Table S3: summary of sequencing reads after filtering. Table S4: summary of genome mapping. Table S5: function annotation statistics table. Table S6: table of statistical results of expression differences. *(Supplementary Materials)*

References

[1] P. Abad, J. Gouzy, J. M. Aury et al., "Genome sequence of the metazoan plant-parasitic nematode *Meloidogyne incognita*," *Nature Biotechnology*, vol. 26, no. 8, pp. 909–915, 2008.

[2] G. Vidal-Diez de Ulzurrun and Y. P. Hsueh, "Predator-prey interactions of nematode-trapping fungi and nematodes: both sides of the coin," *Applied Microbiology and Biotechnology*, vol. 102, no. 9, pp. 3939–3949, 2018.

[3] H. Su, Y. Zhao, J. Zhou et al., "Trapping devices of nematode-trapping fungi: formation, evolution, and genomic perspectives," *Biological Reviews of the Cambridge Philosophical Society*, vol. 92, no. 1, pp. 357–368, 2017.

[4] J. Yang, L. Wang, X. Ji et al., “Genomic and proteomic analyses of the fungus *Arthrobotrys oligospora* provide insights into nematode-trap formation,” *PLoS Pathogens*, vol. 7, no. 9, article e1002179, 2011.

[5] B. L. Wang, Y. H. Chen, J. N. He et al., “Integrated metabolomics and morphogenesis reveal volatile signaling of the nematode-trapping fungus *Arthrobotrys oligospora*,” *Applied and Environmental Microbiology*, vol. 84, no. 9, pp. 1–19, 2018.

[6] L. M. Liang, C. G. Zou, J. Xu, and K. Q. Zhang, “Signal pathways involved in microbe-nematode interactions provide new insights into the biocontrol of plant-parasitic nematodes,” *Philosophical Transactions of the Royal Society B*, vol. 374, no. 1767, p. 20180317, 2019.

[7] K. M. Andersson, T. Meerupati, F. Levander, E. Friman, D. Ahrén, and A. Tunlid, “Proteome of the nematode-trapping cells of the fungus *Monacrosporium haptotylum*,” *Applied and Environmental Microbiology*, vol. 79, no. 16, pp. 4993–5004, 2013.

[8] L. Liang, R. Shen, Y. Mo, J. Yang, X. Ji, and K. Q. Zhang, “A proposed adhesin AoMad1 helps nematode-trapping fungus *Arthrobotrys oligospora* recognizing host signals for life-style switching,” *Fungal Genetics and Biology*, vol. 81, pp. 172–181, 2015.

[9] G. A. M. Cross, “Glycolipid anchoring of plasma membrane proteins,” *Annual Review of Cell Biology*, vol. 6, no. 1, pp. 1–39, 1990.

[10] M. A. Ferguson, “The structure, biosynthesis and functions of glycosylphosphatidylinositol anchors, and the contributions of trypanosome research,” *Journal of Cell Science*, vol. 112, no. 17, pp. 2799–2809, 1999.

[11] F. Elortza, T. S. Nuhse, L. J. Foster, A. Stensballe, S. C. Peck, and O. N. Jensen, “Proteomic analysis of glycosylphosphatidylinositol-anchored membrane proteins,” *Molecular & Cellular Proteomics*, vol. 2, no. 12, pp. 1261–1270, 2003.

[12] M. L. Richard and A. Plaine, “Comprehensive analysis of glycosylphosphatidylinositol-anchored proteins in Candida albicans,” *Eukaryotic Cell*, vol. 6, no. 2, pp. 119–133, 2007.

[13] P. K. Chang, Q. Zhang, L. Scharfenstein et al., “*Aspergillus flavus* GPI-anchored protein-encoding ecm33 has a role in growth, development, aflatoxin biosynthesis, and maize infection,” *Applied Microbiology and Biotechnology*, vol. 102, no. 12, pp. 5209–5220, 2018.

[14] S. Kumar, G. Stecher, and K. Tamura, “MEGA7: molecular evolutionary genetics analysis version 7.0 for bigger datasets,” *Molecular Biology and Evolution*, vol. 33, no. 7, pp. 1870–1874, 2016.

[15] Z. F. Xu, B. L. Wang, H. K. Sun et al., “High trap formation and low metabolite production by disruption of the polyketide synthase gene involved in the biosynthesis of arthrosporols from nematode-trapping fungus *Arthrobotrys oligospora*,” *Journal of Agricultural and Food Chemistry*, vol. 63, no. 41, pp. 9076–9082, 2015.

[16] Z. Zhen, X. Xing, M. Xie et al., “MAP kinase Slt2 orthologs play similar roles in conidiation, trap formation, and pathogenicity in two nematode-trapping fungi,” *Fungal Genetics and Biology*, vol. 116, pp. 42–50, 2018.

[17] X. Yang, N. Ma, L. Yang et al., “Two Rab GTPases play different roles in conidiation, trap formation, stress resistance, and virulence in the nematode-trapping fungus *Arthrobotrys oligospora*,” *Applied Microbiology and Biotechnology*, vol. 102, no. 10, pp. 4601–4613, 2018.

[18] J. Liu, Z. K. Wang, H. H. Sun, S. H. Ying, and M. G. Feng, “Characterization of the Hog1 MAPK pathway in the entomopathogenic fungus *Beauveria bassiana*,” *Environmental Microbiology*, vol. 19, no. 5, pp. 1808–1821, 2017.

[19] B. Langmead and S. L. Salzberg, “Fast gapped-read alignment with Bowtie 2,” *Nature Methods*, vol. 9, no. 4, pp. 357–359, 2012.

[20] B. Li and C. N. Dewey, “RSEM: accurate transcript quantification from RNA-Seq data with or without a reference genome,” *BMC Bioinformatics*, vol. 12, no. 1, p. 323, 2011.

[21] I. Gagnon-Arsenault, L. Parisé, J. Tremblay, and Y. Bourbonnais, “Activation mechanism, functional role and shedding of glycosylphosphatidylinositol-anchored Yps1p at the *Saccharomyces cerevisiae* cell surface,” *Molecular Microbiology*, vol. 69, no. 4, pp. 982–993, 2008.

[22] M. Rabino, L. Trusolino, M. Prat, O. Cremona, P. Savoia, and P. C. Marchisio, “A monoclonal antibody identifies a novel GPI-anchored glycoprotein involved in epithelial intercellular adhesion,” *Journal of Cell Science*, vol. 107, no. 6, pp. 1413–1428, 1994.

[23] C. Liu, J. Xing, X. Cai et al., “GPI7-mediated glycosylphosphatidylinositol anchoring regulates appressorial penetration and immune evasion during infection of Magnaporthe oryzae,” *Environmental Microbiology*, vol. 22, no. 7, pp. 2581–2595, 2020.

[24] S. Ono, “Functions of actin-interacting protein 1 (AIP1)/WD repeat protein 1 (WDR1) in actin filament dynamics and cytoskeletal regulation,” *Biochemical and Biophysical Research Communications*, vol. 506, no. 2, pp. 315–322, 2018.

[25] B. W. Bernstein and J. R. Bamburg, “ADF/cofilin: a functional node in cell biology,” *Trends in Cell Biology*, vol. 20, no. 4, pp. 187–195, 2010.

[26] G. Kanellos and M. C. Frame, “Cellular functions of the ADF/cofilin family at a glance,” *Journal of Cell Science*, vol. 129, no. 17, pp. 3211–3218, 2016.

[27] I. Mabuchi, “An actin-depolymerizing protein (depactin) from starfish oocytes: properties and interaction with actin,” *The Journal of Cell Biology*, vol. 97, no. 5, pp. 1612–1621, 1983.

[28] D. Zhang, X. Zhu, F. Sun, K. Zhang, S. Niu, and X. Huang, “The roles of actin cytoskeleton and actin-associated protein Crn1p in trap formation of *Arthrobotrys oligospora*,” *Research in Microbiology*, vol. 168, no. 7, pp. 655–663, 2017.

[29] K. Zheng, K. Kitazato, Y. Wang, and Z. He, “Pathogenic microbes manipulate cofilin activity to subvert actin cytoskeleton,” *Critical Reviews in Microbiology*, vol. 42, no. 5, pp. 1–19, 2015.

[30] P. Nordenfelt and H. Tapper, “Phagosome dynamics during phagocytosis by neutrophils,” *Journal of Leukocyte Biology*, vol. 90, no. 2, pp. 271–284, 2011.

[31] W. L. Yen and D. J. Klionsky, “How to live long and prosper: autophagy, mitochondria, and aging,” *Physiology (Bethesda)*, vol. 23, no. 5, pp. 248–262, 2008.

[32] Y. L. Chen, Y. Gao, K. Q. Zhang, and C. G. Zou, “Autophagy is required for trap formation in the nematode-trapping fungus *Arthrobotrys oligospora*,” *Environmental Microbiology Reports*, vol. 5, no. 4, pp. 511–517, 2013.

[33] D. J. Hackam, O. D. Rotstein, W. J. Zhang et al., “Regulation of phagosomal acidification: Differential targeting of Na^+/H^+ exchangers, Na^+/K^+-ATPases, and vacuolar-type H^+-ATPases,” *The Journal of Biological Chemistry*, vol. 272, no. 47, pp. 29810–29820, 1997.

[34] P. Saftig and J. Klumperman, "Lysosome biogenesis and lysosomal membrane proteins: trafficking meets function," *Nature Reviews Molecular Cell Biology*, vol. 10, no. 9, pp. 623–635, 2009.

[35] N. Nelson and W. R. Harvey, "Vacuolar and plasma membrane proton-adenosinetriphosphatases," *Physiological Reviews*, vol. 79, no. 2, pp. 361–385, 1999.

[36] H. Wieczorek, D. Brown, S. Grinstein, J. Ehrenfeld, and W. R. Harvey, "Animal plasma membrane energization by proton-motive V-ATPases," *BioEssays*, vol. 21, no. 8, pp. 637–648, 1999.

[37] M. Clarke, J. Köhler, Q. Arana, T. Liu, J. Heuser, and G. Gerisch, "Dynamics of the vacuolar H^+-ATPase in the contractile vacuole complex and the endosomal pathway of *Dictyostelium* cells," *Journal of Cell Science*, vol. 115, no. 14, pp. 2893–2905, 2002.

[38] J. L. Lavín, M. Marcet-Houben, R. L. Gutiérrez-Vázquez et al., "FUNGALOXPHOS: an integrated database for oxidative phosphorylation in fungi," *Mitochondrion*, vol. 13, no. 4, pp. 357–359, 2013.

[39] A. Blomberg and L. Adler, "Physiology of osmotolerance in fungi," *Advances in Microbial Physiology*, vol. 33, pp. 145–212, 1992.

[40] M. Rep, M. Krantz, J. M. Thevelein, and S. Hohmann, "The transcriptional response of *Saccharomyces cerevisiae* to osmotic shock :," *The Journal of Biological Chemistry*, vol. 275, no. 12, pp. 8290–8300, 2000.

[41] G. Yaakov, A. Duch, M. García-Rubio et al., "The stress-activated protein kinase Hog1 mediates S phase delay in response to osmostress," *Molecular Biology of the Cell*, vol. 20, no. 15, pp. 3572–3582, 2009.

[42] Y. Aoki, T. Kanki, Y. Hirota et al., "Phosphorylation of serine 114 on Atg32 mediates mitophagy," *Molecular Biology of the Cell*, vol. 22, no. 17, pp. 3206–3217, 2011.

[43] K. Mao, K. Wang, M. Zhao, T. Xu, and D. J. Klionsky, "Two MAPK-signaling pathways are required for mitophagy in *Saccharomyces cerevisiae*," *The Journal of Cell Biology*, vol. 193, no. 4, pp. 755–767, 2011.

[44] D. Ma and R. Li, "Current understanding of HOG-MAPK pathway in *Aspergillus fumigatus*," *Mycopathologia*, vol. 175, no. 1-2, pp. 13–23, 2013.

[45] G. Boguslawski and J. O. Polazzi, "Complete nucleotide sequence of a gene conferring polymyxin B resistance on yeast: similarity of the predicted polypeptide to protein kinases," *Proc Natl Acad Sci USA*, vol. 84, no. 16, pp. 5848–5852, 1987.

[46] N. Taguchi-Atarashi, M. Hamasaki, K. Matsunaga et al., "Modulation of local PtdIns3P levels by the PI phosphatase MTMR3 regulates constitutive autophagy," *Traffic*, vol. 11, no. 4, pp. 468–478, 2010.

[47] F. L. Robinson and J. E. Dixon, "Myotubularin phosphatases: policing 3-phosphoinositides," *Trends in Cell Biology*, vol. 16, no. 8, pp. 403–412, 2006.

[48] V. Tosch, H. M. Rohde, H. Tronchere et al., "A novel PtdIns*3P* and PtdIns(3,5)P_2 phosphatase with an inactivating variant in centronuclear myopathy," *Human Molecular Genetics*, vol. 15, no. 21, pp. 3098–3106, 2006.

[49] W. R. Parrish, C. J. Stefan, and S. D. Emr, "Essential role for the myotubularin-related phosphatase Ymr1p and the synaptojanin-like phosphatases Sjl2p and Sjl3p in regulation of phosphatidylinositol 3-phosphate in yeast," *Molecular Biology of the Cell*, vol. 15, no. 8, pp. 3567–3579, 2004.